Nonmonotonic Models are Not Necessary to Obtain Shear Banding Phenomena in Entangled Polymer Solutions

J. M. Adams[1] and P. D. Olmsted[2]

[1]*Cavendish Laboratory, University of Cambridge, JJ Thomson Avenue, Cambridge, CB3 0HE, United Kingdom*
[2]*School of Physics & Astronomy, University of Leeds, Leeds, LS2 9JT, United Kingdom*

(Received 6 May 2008; published 12 February 2009)

Recent experiments on entangled polymer solutions may indicate a constitutive instability, and have led some to question the validity of existing constitutive models. We use a modern constitutive model, the Rolie-Poly model plus a solvent viscosity, and show that (i) this simple class of models captures instability, (ii) shear banding phenomena is observable for weakly *stable* fluids in flow geometries with sufficiently inhomogeneous total stress, and (iii) transient phenomena exhibit inhomogeneities similar to shear banding, even for weakly stable fluids.

DOI: 10.1103/PhysRevLett.102.067801 PACS numbers: 61.25.he, 83.50.Ax

Much of the rheology of entangled polymer solutions and melts is captured by the molecular theory of Doi and Edwards (DE) [1], who argued that polymers relax by curvilinear diffusion (reptation) within a tube of the surrounding polymers. The DE model has a local maximum in the constitutive relation (the total shear stress as a function of shear rate for homogeneous flows). The resulting nonmonotonic relation (e.g., the dashed curves in Fig. 2) leads to an instability that for many years was not observed in experiments [2], but nonetheless attracted attention [3,4]. This stress maximum is predicted to be less pronounced or absent if the convected constraint release (CCR) of entanglements due to flow [5–7] is incorporated. A sudden release of a constraint can relax both the orientation and conformation of a stretched polymer, which increases the shear stress and, for sufficiently frequent events, eliminates the instability. The CCR mechanism also leads to neutron scattering predictions that agree with experiment [8]. Similar physics applies to solutions of breakable wormlike micelles, in which the instability is well documented experimentally and leads to *shear banding*, in which a fast-flowing oriented state coexists with a more disordered and viscous state along a stress plateau [9]. There, CCR is less pronounced because of breakage and fails to ameliorate a constitutive instability [7].

Recently, Wang, Hu, and co-workers studied entangled solutions of a high molecular weight (HMW) polymer in its own oligomer [10–13], or DNA solutions [14], finding a number of results that may be consistent with instability and shear banding after all. In controlled shear rate mode a weakly increasing stress plateau of three decades in shear rate was found, whereas in controlled shear stress mode the sheared solution experienced a jump in the shear rate, together with spatially inhomogeneous birefringence [10]. Local velocimetry revealed spatially inhomogeneous velocity profiles in both the transient and the steady state [11] regimes, while large amplitude oscillatory shear flow (LAOS) experiments showed an inhomogeneous banding-like shear rate profile at finite frequencies [15]. Similar behavior was observed in a sliding plate shear cell in monodisperse solutions [12]. Relaxation after a step strain induced a highly inhomogeneous velocity field with *negative* local shear rates [13]. Hu *et al.* found similar inhomogeneous flow behavior and possible signatures of shear banding in polymer solutions, and wormlike micelle solutions at concentrations where severe shear thinning, but not banding, might be expected [16].

Wang *et al.* could not reconcile their results with existing theory, and proposed that the instability is a yield like effect due to an unbalanced ''entropic retraction force'' [17]. Here we show that much of the phenomenology of these experiments is consistent with the predictions of tube models with CCR, perhaps as anticipated in the original theory [3], without introducing new physics.

Model.—We separate the total stress $\mathbf{T}$ into a fast Newtonian (or solvent) stress and a slow viscoelastic stress $\mathbf{\Sigma}$ (HMW polymer):

$$\mathbf{T} = -p\mathbf{I} + 2\eta\mathbf{D} + G\mathbf{\Sigma}, \tag{1}$$

where $\mathbf{I}$ is the identity tensor, $\mathbf{D} = \frac{1}{2}[\nabla\mathbf{v} + (\nabla\mathbf{v})^T]$, incompressibility determines the pressure p, and η is the solvent viscosity. We define the dimensionless quantity $\epsilon = \eta/(G\tau_d)$, where τ_d is the reptation time, and study the creeping flow limit $\nabla \cdot \mathbf{T} = 0$. We use the Rolie-Poly (RP) model [6], a simplified tube model that incorporates CCR [7], for the dynamics of $\mathbf{\Sigma}(\mathbf{r}, t)$:

$$(\partial_t + \mathbf{v}\cdot\nabla)\mathbf{\Sigma} - (\nabla\mathbf{v})\cdot\mathbf{\Sigma} - \mathbf{\Sigma}\cdot(\nabla\mathbf{v})^T + \frac{1}{\tau_d}\mathbf{\Sigma} = 2\mathbf{D} - \frac{2}{\tau_R}(1-A)[\mathbf{I} + \mathbf{\Sigma}(1+\beta A)] + \mathcal{D}\nabla^2\mathbf{\Sigma}, \tag{2}$$

where $A = (1 + \mathrm{tr}\mathbf{\Sigma}/3)^{-1/2}$ and the Rouse time τ_R governs chain stretch. The stress ''diffusion'' term $\mathcal{D}\nabla^2\mathbf{\Sigma}$ describes the

response to an inhomogeneous viscoelastic stress; while not in the original RP model, it can arise due to diffusion or finite persistence length [18–20]. We specify Neumann boundary conditions ($\nabla\boldsymbol{\Sigma} = 0$) [20,21].

From experimental values of the plateau modulus $G \sim 6 \times 10^2$ Pa, reptation time $\tau_d \sim 20$ s, and solvent viscosity $\eta \sim 1$ Pa s [10], we use $\epsilon = 10^{-5}$. Here we use $\tau_d/\tau_R \sim 10^3$, which is consistent with the length of the stress-shear rate plateau reported in [10]. The parameter β controls the efficiency of CCR, and its value is not yet agreed upon. Reference [6] chose $\beta = 1$ to fit steady state data in polymer melts, and used multiple modes with $\beta = 0.5$ to fit experimental transient data. Here we tune between two qualitatively different types of constitutive curve, either a nonmonotonic (0.65) or a monotonic (0.728) constitutive curve with a broad plateau (Figs. 1 and 2).

Equation (2) was solved in one spatial dimension using the Crank-Nicolson algorithm [18], for unidirectional Couette flow $v(r, t)\hat{\theta}$ between cylinders of radii R_1 and R_2 parameterized by $q \equiv \ln(R_2/R_1)$. In this geometry the total shear stress $T_{r\theta} \sim 1/r^2$, so that the stress difference across the flow cell is $\Delta \ln T_{r\theta} = 2q$. Cone and plate flow with cone angles of $\theta = (4°, 1°)$ has been reported [11,16], so we use consistent values of stress difference corresponding to $q \simeq \Delta R/R = (2 \times 10^{-3}, 2 \times 10^{-4})$ [20]. Stresses are measured in units of G, shear rates in units of τ_d^{-1}, and velocities in units of $qR_1/\tau_d \approx \Delta R/\tau_d$ for small q. To plot numerical data we use Γ, the dimensionless specific torque (per height per radian) on the inner cylinder. The diffusion constant used was $\mathcal{D}\tau_d/(R_1 q)^2 = 4 \times 10^{-4}$.

Flow curves.—To calculate the steady state flow curves a step shear rate was applied from rest and evolved for $500\tau_d$ with time step $10^{-5}\tau_d$, after which subsequent shear rate steps and time evolutions were applied to scan up and down in shear rate (Fig. 2). For nonmonotonic constitutive curves ($\beta = 0.65$) shear banding always occurs, with hysteresis and a stress "plateau." For the monotonic case ($\beta = 0.728$) shear banding could be inferred in the more highly curved geometry with the larger stress difference (larger q), since the flow curve no longer follows the constitutive curve, but *without* hysteresis. Crudely, a monotonic flow curve exhibits bandinglike flows when most of the shear rate in the gap occurs over a small range of stresses; i.e., the slope of the plateau must be much smaller than the apparent slope specified by the flow geometry:

$$\left.\frac{d\Gamma}{d\dot{\gamma}}\right|_{\text{C.C.}} \ll \left.\frac{\Gamma(R_1) - \Gamma(R_2)}{\Delta\dot{\gamma}}\right|_{g} \sim e^q - 1, \qquad (3)$$

where "C.C." denotes the flat portion of the constitutive curve (dashed in Fig. 2) and "g" refers to the range of torques and shear rates specified by the flow geometry.

The steady state velocity profiles are shown in Fig. 3 as solid (red) lines. The nonmonotonic flow curves ($\beta = 0.65$) lead to a pronounced kink in the velocity profile, a signature of shear banding. The monotonic case does not shear band in the flatter geometry (small q), but for a more curved geometry (larger q) more shear rates are accessible and the resulting smooth velocity profile could easily be interpreted as banding [11]; certainly the constitutive curve is not followed (Fig. 2). Similar smooth profiles were reported in [11,16], in a flow geometry with $q \simeq 0.004$–0.02. A slightly increasing stress plateau over several decades in shear rates (as in [10]) would thus lead to apparently banding (inhomogenous) flow in geometries with small stress gradients, but homogeneous flow obtains for sufficiently small q [Eq. (3)].

Start-up transients.—Transients were studied by evolving from rest using a time step of $10^{-5}\tau_d$ (Fig. 3). In all cases shown here strongly inhomogeneous flow develops after the stress overshoot, leading to a sharply banded transient state, with a *negative* velocity and shear rate in the less viscous band. In the monotonic case the velocity profile eventually smooths out. For a narrower stress pla-

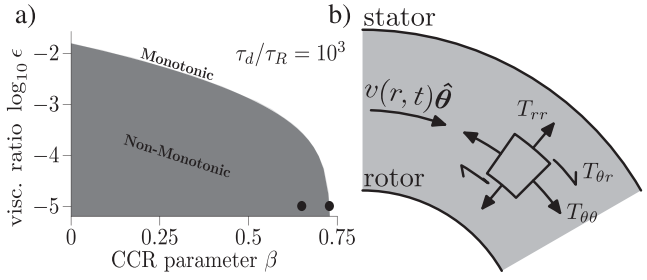

FIG. 1. (a) Parameters (β, ϵ) where the constitutive curve of the Rolie-Poly model is nonmonotonic (shaded). (b) Section through Couette rheometer showing the flow field and total stress components, **T**.

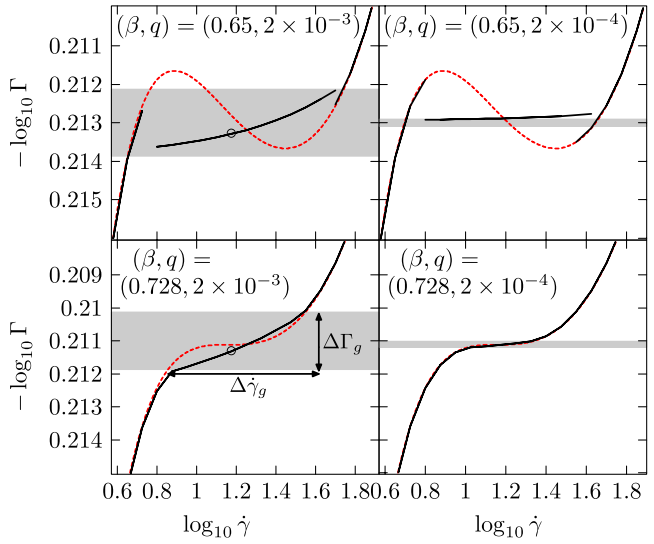

FIG. 2 (color online). Flow curves (solid black) and constitutive curves (dashed red) for a range of stress gradients q and CCR values β. The shaded area shows the size of the torque difference $\Delta\log_{10}\Gamma = \log_{10}e^{2q}$. Circles indicate applied shear rates at which the transient state responses are shown in Fig. 3.

teau (e.g., $\beta = 0.3$, not shown) the overshoot has a less pronounced kink and typically a positive shear rate. We have found inhomogeneous transients with negative velocities with stress differences corresponding to a cone angle $\theta = 0.003°$, while for $\theta = 0.001°$ the inhomogeneous strain rate is no longer negative, and for $\theta = 0°$ the flow remains homogeneous. With perturbed initial conditions then the inhomogeneous transient behavior returns. The transient for a monotonic model ($\beta = 0.728$) in which spatial gradients are artificially prohibited exhibits a slower decrease after the stress overshoot than in the spatially resolved model (Fig. 3); hence, inhomogeneities are important when using transient data to help differentiate candidate constitutive models [1,22].

Large amplitude oscillatory shear (LAOS).—A sinusoidal spatially averaged shear rate was applied with frequency Ω and maximum shear rate $\dot{\gamma}_m$, and evolved from rest (zero stress) until initial transients decayed. We characterize the dynamics by the Deborah ($\mathrm{De} = \Omega\tau_d$) and Weissenberg ($\mathrm{Wi} = \dot{\gamma}_m\tau_d$) numbers. Low De (frequency) should lead to some features of the steady state behavior, such as transient banding for Wi roughly within the nonmonotonic part of the flow curve, while higher frequencies (De) should produce sharper profiles similar to the transient behavior in Fig. 3, since the system cannot relax before flow reversal. At the highest frequencies the fast reversing dynamics should prohibit an inhomogenous state.

Figure 4(a) shows this behavior on a "Pipkin diagram" of Wi vs De, for a monotonic flow curve ($\beta = 0.728$) in a slightly curved geometry. The inhomogeneous profiles in the banding regime [Fig. 4(d)] can be represented parametrically in terms of shear rate and torque, $(\dot{\gamma}(y), \Gamma(y))$ [Fig. 4(b)]. At the high stress regions of the cycle a portion of the sample enters the high shear rate band as reported experimentally [22]. In these calculations the position y_* of the interface at a given strain $\dot{\gamma}_0/\Omega = 3$ varied with De as $y_* \sim (\mathrm{De})^{\alpha}$, where $\alpha \sim 0.4$–0.6, unlike the fixed position reported in Ref. [15]. We suspect that these experiments did not attain steady state. The torque overshoot is typical of polymer solutions, like that found in [16] (Fig. 4). At low frequencies the system has time to find a selected stress, which remains constant while the shear band grows into the cell. At high frequencies the fluid cannot relax or shear band, which leads to a sinusoidal response and a nearly affine spatial profile.

Step strain.—Some step strain experiments found a strong inhomogeneous recoil that developed a negative velocity gradient [13]. We illustrate this for a monotonic constitutive curve ($\beta = 0.728$), Fig. 5. As in Fig. 5 of [13], an inhomogeneous velocity profile develops and the velocity becomes negative as the system recoils. Experimentally, the total displacement after recoil is of the order

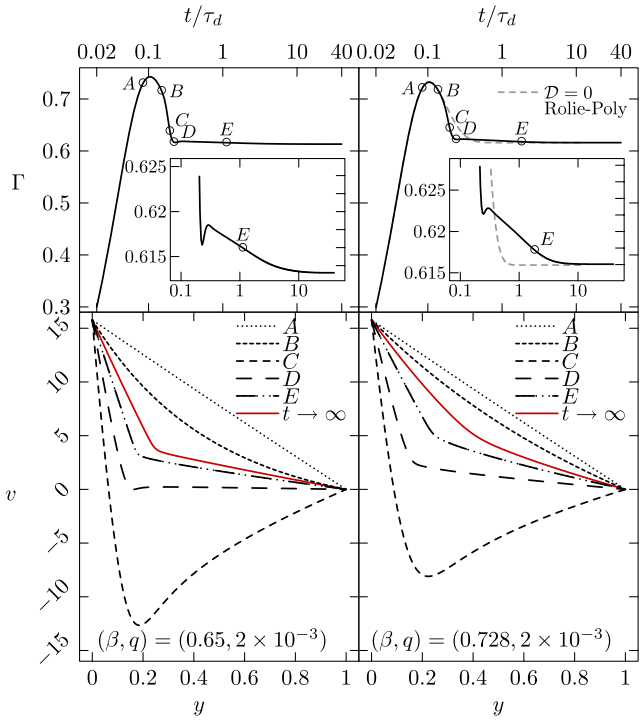

FIG. 3 (color online). Velocity as a function of position $y = q^{-1}\ln(r/R_1)$ for different (β, q), at shear rate $\log_{10}\dot{\gamma} = 1.2$ (○ in Fig. 2). The solid (red) lines indicate the steady state profile, and dashed lines are transient profiles at the times shown. The transient torque response $\Gamma(t)$ in the spatially uniform model is shown for the monotonic case ($\beta = 0.728$) by a dashed line.

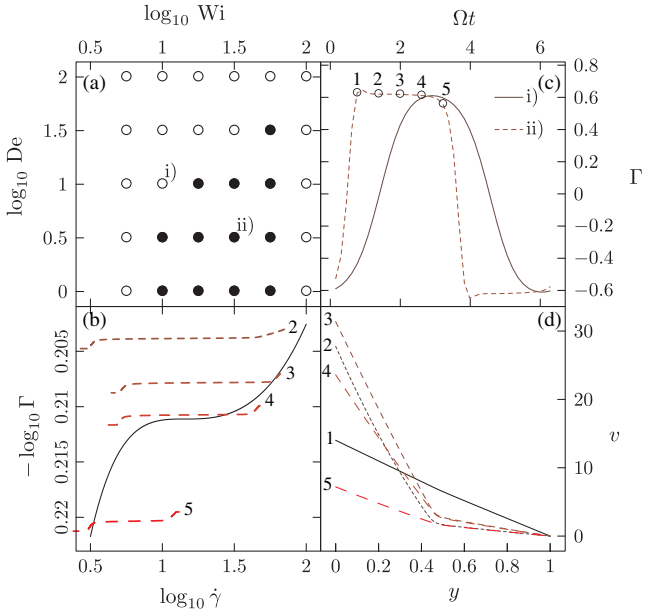

FIG. 4 (color online). (a) Pipkin diagram (Wi vs De) for $\beta = 0.728$ and $q = 2 \times 10^{-3}$, showing regions with homogeneous (○) and inhomogeneous profiles (●). (b) Parametric shear rate—torque profiles $(\dot{\gamma}(y), \Gamma(y))$ (dashed lines: 3,4) overlaying the constitutive curve (solid). (c) Torque evolution for different De noted on (a). (d) Velocity profiles for ii); profiles (1–5) are at different times in the cycle for $\mathrm{De} \simeq 3$ (ii) [○ in (c)].

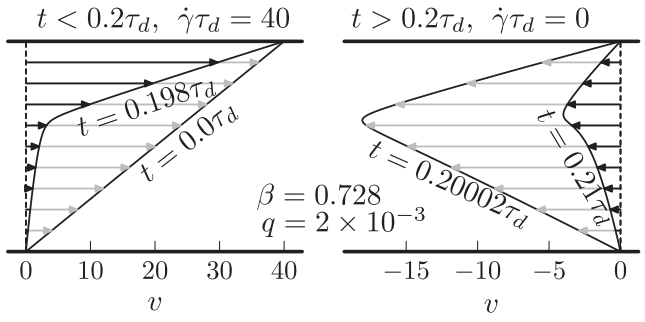

FIG. 5. Relaxation of a step strain of $\gamma = 8$, applied using $\dot{\gamma}\tau_d = 40$ for $t = 0.2\tau_d$. (Left) Velocity before the shear rate stops and (right) snap shots of recoil velocities.

of a tenth of the gap size which is comparable with that observed here. Thus, inhomogeneous flow must be considered when using step strain data to help discriminate among candidate constitutive models, as when using the DE damping function [1,22].

Summary.—We have shown that behavior reminiscent of shear banding, as reported recently, can be reproduced using the Rolie-Poly model supplemented by a term to accommodate spatial gradients. The RP model contains an unknown parameter β, which controls the efficacy of convected constraint release. Even for β large enough to yield a stable (monotonic) constitutive curve, shear banding signatures can appear if the "stress plateau" is flat enough: (i) a geometry with a high stress gradient can induce a flow profile that could be mistaken for banding; (ii) sharp bandinglike profiles can appear in start-up transients even though the steady state is nonbanded; (iii) LAOS can trap these sharp transient profiles; and (iv) relaxation after a large step strain can be very inhomogeneous, sometimes with a negative shear rate recoil. Several recent experiments, particularly on polydisperse polymer solutions, may fall into this category [16]. A wide plateau is believed to accompany very highly entangled systems [7], and the larger number of relaxation times are likely to render polydisperse systems intrinsically more stable than monodisperse systems [3], as was noted in recent experiments [16]. Our results are not specific to the RP model; Zhou *et al.* recently studied a different two-fluid model of shear banding (with a nonmonotonic constitutive relation), and found qualitative results similar to some of ours [23].

We thank S.-Q. Wang, R. Graham, T. McLeish, O. Radulescu, and S. Fielding for lively discussions. This work was supported by the Royal Commission of 1851.

[1] M. Doi and S. F. Edwards, *The Theory of Polymer Dynamics* (Clarendon, Oxford, 1989).

[2] R. A. Stratton, J. Colloid Interface Sci. **22**, 517 (1966); E. V. Menezes and W. W. Graessley, J. Polym. Sci., Polym. Phys. Ed. **20**, 1817 (1982); C. A. Hieber and H. H. Chiang, Rheol. Acta **28**, 321 (1989); C. Pattamaprom and R. Larson, Macromolecules **34**, 5229 (2001).

[3] M. Doi and S. Edwards, J. Chem. Soc., Faraday Trans. **75**, 38 (1979).

[4] T. C. B. McLeish and R. C. Ball, J. Poly. Sci., B, Polym. Phys. **24**, 1735 (1986); T. C. B. McLeish, J. Poly. Sci., B, Polym. Phys. **25**, 2253 (1987).

[5] G. Marrucci, J. Non-Newtonian Fluid Mech. **62**, 279 (1996); D. W. Mead, R. G. Larson, and M. Doi, Macromolecules **31**, 7895 (1998); G. Ianniruberto and G. Marrucci, J. Non-Newtonian Fluid Mech. **95**, 363 (2000).

[6] A. E. Likhtman and R. S. Graham, J. Non-Newtonian Fluid Mech. **114**, 1 (2003).

[7] S. T. Milner, T. C. B. McLeish, and A. E. Likhtman, J. Rheol. (N.Y.) **45**, 539 (2001).

[8] J. Bent, L. R. Hutchings, R. W. Richards, T. Gough, R. Spares, P. D. Coates, I. Grillo, O. G. Harlen, D. J. Read, and R. S. Graham, *et al.*, Science **301**, 1691 (2003).

[9] N. A. Spenley, M. E. Cates, and T. C. B. McLeish, Phys. Rev. Lett. **71**, 939 (1993); M. E. Cates and S. M. Fielding, Adv. Phys. **55**, 799 (2006).

[10] P. Tapadia and S. Q. Wang, Phys. Rev. Lett. **91**, 198301 (2003).

[11] P. Tapadia and S. Q. Wang, Phys. Rev. Lett. **96**, 016001 (2006).

[12] P. E. Boukany and S.-Q. Wang, J. Rheol. (N.Y.) **51**, 217 (2007).

[13] S.-Q. Wang, S. Ravindranath, P. Boukany, M. Olechnowicz, R. Quirk, A. Halasa, and J. Mays, Phys. Rev. Lett. **97**, 187801 (2006).

[14] P. E. Boukany, Y. T. Hu, and S. Q. Wang, Macromolecules **41**, No. 7, 2644 (2008).

[15] P. Tapadia, S. Ravindranath, and S. Q. Wang, Phys. Rev. Lett. **96**, 196001 (2006).

[16] Y. T. Hu, L. Wilen, A. Philips, and A. Lips, J. Rheol. (N.Y.) **51**, 275 (2007); Y. T. Hu, C. Palla, and A. Lips, J. Rheol. (N.Y.) **52**, 379 (2008).

[17] S.-Q. Wang, S. Ravindranath, Y. Wang, and P. Boukany, J. Chem. Phys. **127**, 064903 (2007); Y. Wang, P. Boukany, S.-Q.Wang, and X. Wang, Phys. Rev. Lett. **99**, 237801 (2007).

[18] P. D. Olmsted, O. Radulescu, and C.-Y. D. Lu, J. Rheol. (N.Y.) **44**, 257 (2000).

[19] A. W. El-Kareh and L. G. Leal, J. Non-Newtonian Fluid Mech. **33**, 257 (1989).

[20] J. M. Adams, S. M. Fielding, and P. D. Olmsted, J. Non-Newtonian Fluid Mech. **151**, 101 (2008).

[21] A. V. Bhave, R. C. Armstrong, and R. A. Brown, J. Chem. Phys. **95**, 2988 (1991).

[22] S. Ravindranath and S. Q. Wang, Macromolecules **40**, 8031 (2007).

[23] L. Zhou, P. A. Vasquez, L. P. Cook, and G. A. McKinley, J. Rheol. (N.Y.) **52**, 591 (2008).